ASSESSMENT OF DEFECTS IN WIND AND TIDAL TURBINE BLADES USING GUIDED WAVES

Kena Makaya*, Kenneth Burnham**, Carmen Campos**

Wind and tidal energy are increasingly important contributors of power within the renewable energy sector. In recent years there have been an increasing number of reports of defective blades contributing towards turbine failure. Within the larger blade designs, a composite structure of glass fibre reinforced plastic (GFRP) or carbon fibre reinforced plastic (CFRP) provides support - termed a *Shear Web* or *Spar Box*. Disbond between the inner shell and bonding flange of the support is not uncommon. Other defects include delamination between the laminate plies that comprise the support structure and structural damage due to impact. Guided Wave Testing (GWT) is a non-destructive testing technique which enables the detection of defects for in-service inspection. This study analyses the signals of Lamb waves propagating within GFRP laminates, and the signal response when they interact with a disbond, present between CFRP and GFRP structures. The results of the study will benefit the design of an array of sensors for an in-situ inspection.

Key words: GWT, Lamb waves, Polymer matrix composites, Disbond.

INTRODUCTION

In February 2009, the United Kingdom (UK) recorded a 38% increase in the total installed capacity (3,331 MW) for wind energy generation, above 2007 levels [1]. Furthermore, the UK is now the world leader in offshore wind energy with 598MW capacity. The UK government has set a target to obtain 20% of electricity from renewable sources by 2020 with wind energy expected to be the biggest contributor.

Cost analysis of wind power remains uncertain. Operational and maintenance (O&M) costs for new large turbines are rarely reported. An analysis by Rademakers et al., [2], disclosed that 60% of turbine lifecycle cost comprised component parts and, of those parts, the rotor and the nacelle absorbed 30% of the total cost each.

* Long Range Ultrasonic (LRU) Section, TWI, Granta Park, Great Abington, Cambridge, UK, CB21 6AL; School of Metallurgy and Materials, University of Birmingham, Edgbaston, Birmingham, B15 2TT

** Long Range Ultrasonic (LRU) Section, TWI, Granta Park, Great Abington, Cambridge, UK, CB21 6AL

Further analysis on maintenance costs attributed 34% of all downtime to the rotor blade. Although this provides little more than an indication of the overall O&M costs, it is sufficiently significant to consider non-destructive testing (NDT) for wind-turbine blades.

Typical rotor blades are made from a composite construction of glass fibre, resin (epoxy, acrylic or phenolic) and possibly wood. Figure 1 illustrates typical cross-section views of two blades incorporating a strengthening member known as a *shear web* or *spar box*, extending from the rotor hub to the tip of the blade.

Composite materials can be degraded in service by a number of mechanisms dependent upon the environment and the sensitivity of the materials used. The mechanisms of degradation include static overload, impact, fatigue, overheating, lightning strike and creep. However, although the mechanisms by which defects are initiated and grow are varied, only a small number of different types of defect result: fracture or buckling of fibres, failure of the interface between the fibres and matrix, cracks, delaminations, bond failures and ingress of moisture, [3].

Turbine blades are largely inaccessible and thus any inspection area must be suitable for long-term automated monitoring. Although details of blade defects are exceptionally difficult to obtain, problems involving the blade support structure have been reported by maintenance and repair companies, [4] . Long Range Ultrasonic Testing (LRUT) is an NDT technique that uses low frequency guided waves and is most commonly used to inspect pipelines [5]. It is particularly suitable as a tool to inspect large areas such as the shear web. The LRUT technique has been widely accepted as a NDT screening technique since the 1990s. It has been mainly used for assessing metallic structures and researchers are now focusing on the performance of the technique on composite materials.

GUIDED WAVES

In plate-like structures (where material thickness is comparable to the ultrasound wavelength) it is possible to propagate guided waves parallel to the plate surfaces. Lamb waves travel through the entire thickness of the material and can propagate for considerable distances in plates, thus making it possible to detect flaws over a sizable area with a single transducer (or several transducers). For a plate of given thickness, there exists a finite number of symmetrical and anti-symmetrical waves within a specific frequency range, each differing from the others by its phase and group velocities and distribution of the displacements and stresses throughout the thickness of the plate [7].

Different types of defect will typically exhibit different signal characteristics on inspection, thus providing a potential mechanism for discrimination. Considering the propagation of such signals in a rotor blade structure, it is important to note that the effects of the material boundaries will have a major impact on the nature of the energy propagation. Typically, guided ultrasonic wave modes will be established, and in order to predict the nature of the output waveform monitored by the reception transducer, it is important to understand the multi-mode and dispersive properties of such waves within a specific material.

Dispersion can be controlled by careful selection of the propagating mode. Physical energy loss, through material damping and viscoelastic effects is material and frequency dependent (increasing rapidly with frequency) and can be addressed through control of the excitation (and/or monitored) frequency band. Effects due to the anisotropic nature of typical composite materials may involve energy being guided in unexpected (and possibly unwanted) directions due to the lay-up of the material.

EXPERIMENTAL RESULTS

Three different test samples were manufactured: two glass fibre reinforced plastic (GFRP) plates and one specimen which is a blade mock-up featuring a spar-cap bonded to a shell. The spar cap section predominantly comprises layers of CFRP with occasional interleaving of GFRP layers. The shell or base panel comprises GFRP material only.

The first GFRP plate tested, dimensions 2000mm x 1000mm x 4mm, exhibited a quasi-isotropic fibre orientation (0º, 90º/±45º) with 6 plies. The sample lay-up is detailed in Table 1.

Table 1: Stacking sequence for the quasi-isotropic sample

Ply number	Orientation of layers
1	Woven (0º/90º)
2	Biaxial (± 45º)
3	Woven (0º/90º)
4	Woven (0º/90º)
5	Biaxial (± 45º)
6	Woven (0º/90º)

Analysed at Kaunas University of Technology (KTU), a low frequency ultrasonic measurement system (ULTRALAB), was used in combination with a single-axis scanner and adjustable transducer holders. PZT transducers were coupled to the structure with glycerol as shown in Figure 2.

The applied signal was a Hann-windowed 100kHz sine-wave with amplitude $100V_{Peak\text{-}to\text{-}Peak}$ and gain 10dB. The tests were performed such that the line of propagation between the transmitter and the receiver was parallel to the on-fibre (0º, 45° or 90°) directions. The fixed transmitter was placed at a distance of 250mm from the receiver starting position, which was then incrementally moved towards the transmitter in 1mm steps, covering a distance of 200mm. The data was analysed using MatLab where a two-dimensional Fast Fourier Transform (2DFFT) was used to ascertain the presence of Lamb wave modes propagating within the sample. The 2DFFT assumes that the surface function has been sampled in the *x* dimension with sample interval T_x and sampled in the y dimension with sample interval T_y. The resulting sampled 2DFFT function is $h(pT_x, qT_y)$ where $p = 0,1,\ldots,N-1$ and $q = 0,1,\ldots,M-1$, [8]:

$$H\left[n/NT_x, m/MT_y\right] = \sum_{q=0}^{M-1}\sum_{p=0}^{N-1} h\left[pT_x, qT_y\right] e^{-j2\pi\left(\frac{mq}{M}+\frac{np}{N}\right)} \quad \text{Eq 1}$$

Where *h* represents the continuous 2DFFT function of the spatial and temporal data, and *H* represents the sampled function. Figure 3 illustrates the dispersion curves, for the quasi-isotropic GFRP plate, over a

normalised frequency-thickness scale. For the purposes of repeatability, three separate tests were performed (blue, red and green traces). Two Lamb wave modes were observed: the fundamental symmetrical mode, S_0, and the fundamental anti-symmetric mode, A_0.

A similar analysis was conducted on a bidirectional, 1300mm x 1000mm x 7.4 mm, GFRP sample comprising 16 plies, with 0º/90º fibre orientation. The dispersion curves related to this specimen (over a normalized frequency-thickness scale) are presented in Figure 4.

Comparing Figure 3 with Figure 4 in the frequency range 0-300kHz, it is observed that the quasi-isotropic sample exhibits the propagation of the fundamental Lamb wave modes only, as opposed to fundamental and higher order wave modes propagating in the bidirectional sample. The difference in the number of wave modes, propagating though the two distinctive samples, may be due to the different ply lay-up resulting in dissimilar elastic stiffness constants (C_{ijkl}).

To better observe the relationship between the propagation of the fundamental Lamb wave modes (A_0 and S_0) and the orientation of the fibres, an experiment was conducted on each sample (Quasi-isotropic and bidirectional GFRP) to obtain the respective group velocity plots. Each specimen was cut into a circular shape with a diameter of 1m and marked into 5° divisions. The test was performed in the laboratory at TWI, using the Teletest® Focus unit and two M2814-P1 types Macro-Fibre Composites (MFCs) sensors. The dimensions of the active area within the sensor are 28mm x 14mm. The transmitter was placed at the centre of the plate and the receiver was placed close to the edge of the sample. The MFCs were coupled to the composite sample using 4kg weights and a metal 'spacer' of 475 mm long, for uniform spacing between the transmitter and the receiver. The centre frequency for the sensor response was 48kHz for the quasi-isotropic sample and 56kHz for the bidirectional one. The experimental set-up is illustrated in Figure 5.

Previous work conducted on a 2mm 2-ply bi-directional GFRP sample suggested that an S_0 group velocity of approximately 4000ms^{-1} and an A_0 group velocity of approximately 1000ms^{-1} at 50kHz, [6]. The group velocities of the S_0 mode in the quasi-isotropic and bidirectional materials are illustrated in Figure 6 and 7 respectively.

For the quasi-isotropic specimen, an S_0 group velocity of approximately 3000ms^{-1} and an A_0 group velocity of approximately 1050m/s were measured for each radius around the plate circumference. For both wave modes, the measured group velocity is largely independent of the fibre orientation of the plate and this is likely due to the fact that a quasi-isotropic material has similar mechanical characteristic as that of an isotropic material.

For the bidirectional plate, an S_0 group velocity of approximately 3000ms^{-1} and an A_0 group velocity of approximately 1100ms^{-1} were measured for each radius around the plate circumference. The directions along which the fibres are aligned (i.e. 0°/90°/180°/270°) produced a maximum S_0 group velocity of 3000ms^{-1}. Deviation in propagation direction from these specific angles (i.e. off-fibre) shows the group velocity falling to a minimum of 1000ms^{-1}. These results are in agreement with the work conducted by Rhee [9] where the S_0 was reported as being dependent on fibre orientation in bidirectional plates, and independent of fibre orientation in the quasi-isotropic specimens. However, it is observed that the S_0 group velocity value varies significantly from the 4000ms^{-1} previously measured and that is most likely due to the difference in ply lay-up and manufacturing processes.

To exploit further the propagation of the S_0 and A_0 wave modes, their behaviour was examined within a blade mock-up sample featuring a disbond between two components: the base panel comprising a GFRP bidirectional plate, 8 mm-thick featuring16 plies. The first ply was oriented at 0º and the second ply oriented at 45º, a sequence repeated up to ply number 16. The spar-cap comprised predominantly of CFRP plies (all oriented at 0°) with occasional GFRP plies interleaved (and oriented at 45°). In total, the spar cap comprised 33 plies at a thickness of 40 mm.

An array of 4 transmit MFCs and 4 receive MFCs were symmetrically placed at either side of the disbond across the width of the sample, as shown in Figure 10. The centre frequency was measured as 56kHz. Results are presented in Figure 11.

The disbond was successfully detected and the scan image shows that the disbond is not uniform across the spar cap. The scale in colour in Figure 11 represents the signal amplitude in mV. There were 44 separate scans recorded. Each scan represents the array, 80 mm long, being displaced by a 10mm increment in the rightwards direction. Test No. 1 through to 6 and Test No. 39 onwards, data is recorded where there is no coverage of the disbond by the array. For Test No. 7 through to 13, and Test No. 32 through to 38 partial coverage of the defect was achieved. For Test No 14 through to 31, full-coverage of the disbond by the array was achieved. However, it is observed that S_0 and A_0 magnitude measured by the array is not constant for the full length of the disbond, suggesting that the array needs to be further optimized and / or the disbond is not wholly complete. In addition, the S_0 mode exhibits the highest signal amplitude when propagating through the disbond, and thus detecting more of the disbond than the A_0 mode. Although there are no known defects prior to test location No. 6 and beyond test location No. 31, indications of a 'defect' (other than the disbond) are observed although with very small signal amplitudes. Further NDT inspections (ultrasonic testing or infrared thermography) will need to be carried to assess whether this specimen contains additional manufacturing defects.

CONCLUSION AND FUTURE WORK

Dispersion curves were produced that show more propagating wave modes in the GFRP bidirectional sample than in the GFRP quasi-isotropic sample. The fundamental Lamb wave modes (S_0 and A_0) were independent of fibre orientation in the quasi-isotropic specimen whilst the bidirectional sample exhibited S_0 mode behaviour dependent on fibre orientation. In addition, the S_0 mode appears to be sensitive to the different stacking sequences when comparing both specimens as both GFRP plates differ in fibre orientation, lay-up and thickness.

A blade sample manufactured from two different material types (GFRP, CFRP) featured a disbond of 250mmx250mm. The transmitting and receiving MFC arrays were able to clearly detect this defect. The magnitudes of the recorded signals, as observed in an image-scan, were not constant suggesting that the disbonded area might not have been uniform. The size of the MFC array could have had an influence on the amount of energy transmitted in the structure, suggesting that further optimization of the array is required in order to improve the signal-to-noise ratio.

In order to achieve a successful array design, it is important to know the exact wavelength of wave mode to be transmitted in the material. Determining the wavelength of wave modes will help in selecting desired modes and cancelling unwanted ones within the material. Both S_0 and A_0 modes appeared to be suitable for the detection of disbond type defects. Future work will focus on the sensitivity of S_0 and A_0 modes to detect smaller disbond areas. The sensor array will be optimsed to preferentially excite the most sensitive mode suitable for the detection of composite defects.

ACKNOWLEDGEMENTS

Kena Makaya is studying for an Engineering Doctorate at the University of Birmingham under the sponsorship of EPSRC and TWI Ltd. The work was carried out under the 'In-situ Monitoring of on- and offshore Wind Turbine Blades Using Energy Harvesting Technology' and 'Development of a Condition

Monitoring System for Tidal Stream Generator Structures' projects, funded by the European Commission within the Framework 7 Programme.

WINTUR is collaboration between the following organisations: TWI LIMITED, OPTEL sp.Z o.o., SMART MATERIAL GmbH, CEDRAT Technologies, MIYAMA COMPOSITES Ltd, ENCOCAM Limited, SOLENT COMPOSITE SYSTEMS Ltd, SOUTHERN & SCOTTISH ENERGY, CERETETH, KAUNAS UNIVERSITY OF TECHNOLOGY. The Project is co-ordinated and managed by TWI Ltd. and is partly funded by the EC under the Research for the benefit of SMEs programme. Grant Agreement Number 232190.

TIDALSENSE is collaboration between the following organisations: TWI LIMITED, CERETETH, ENEROCEAN, I&T NARDONI, IKNOWHOW, INNOTEC, IT POWER, KAUNAS UNIVERSITY OF TECHNOLOGY, TIDALSAILS. The research leading to these results has received funding from the European Union's Seventh Framework Programme managed by REA-Research Executive Agency http://ec.europa.eu/research/rea [FP7/2007-2013] under Grant Agreement Number 232518.

FIGURES

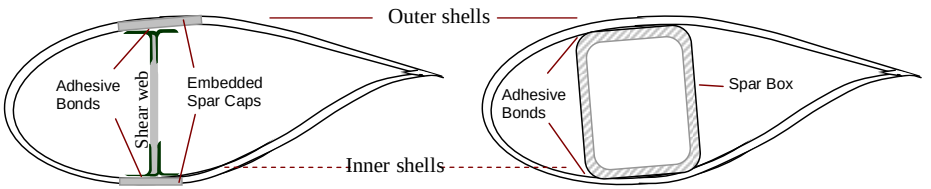

Figure 1: Typical Rotor Blade cross-sections

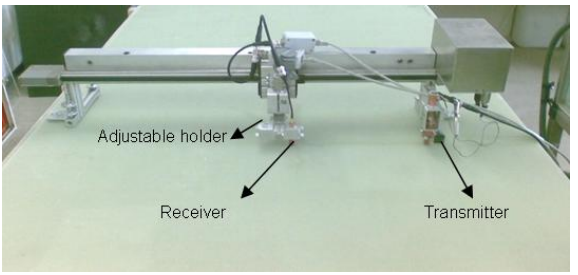

Figure 2: Experimental set-up

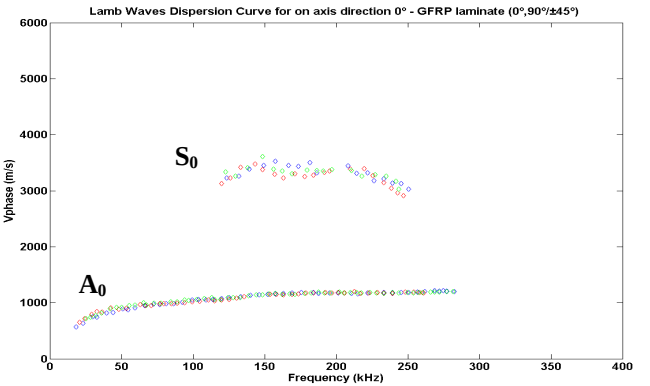

Figure 3: Normalised Dispersion curve - quasi-isotropic sample

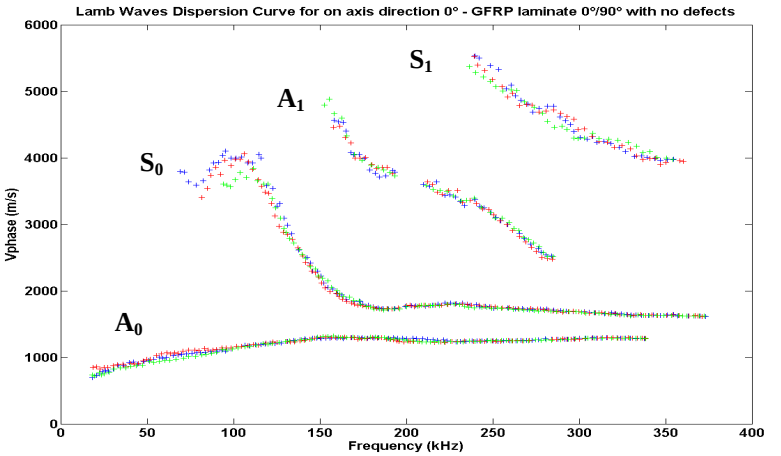

Figure 4: Normalised dispersion curve – bidirectional sample

Figure 5: Circular GFRP sample with 5 degree division (top) and with MFCs applied (bottom)

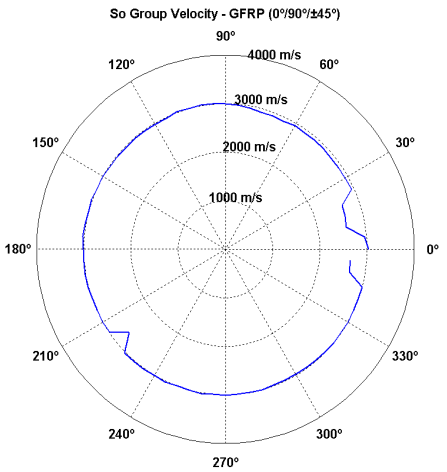

Figure 6: S_0 group velocity in the quasi-isotropic GFRP

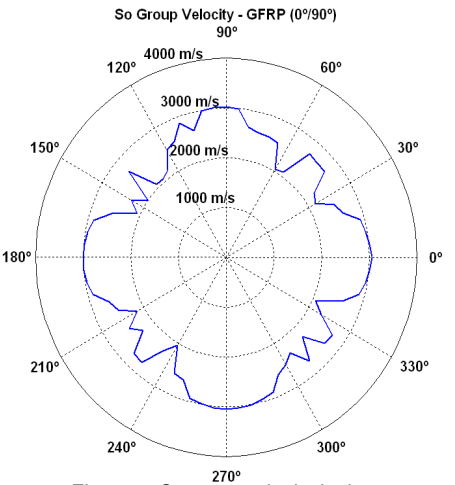

Figure 7: S_0 group velocity in the bidirectional GFRP

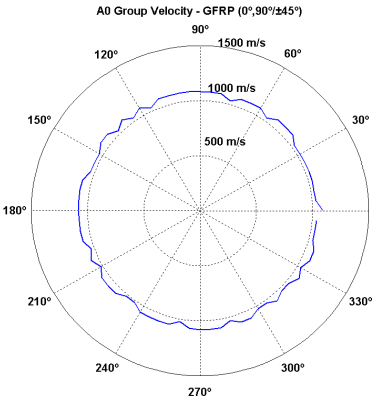

Figure 8: A_0 group velocity in the quasi-isotropic GFRP

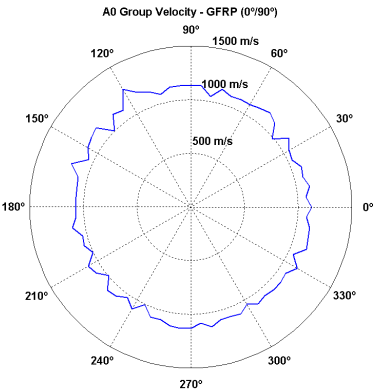

Figure 9: A_0 group velocity in the bidirectional GFRP

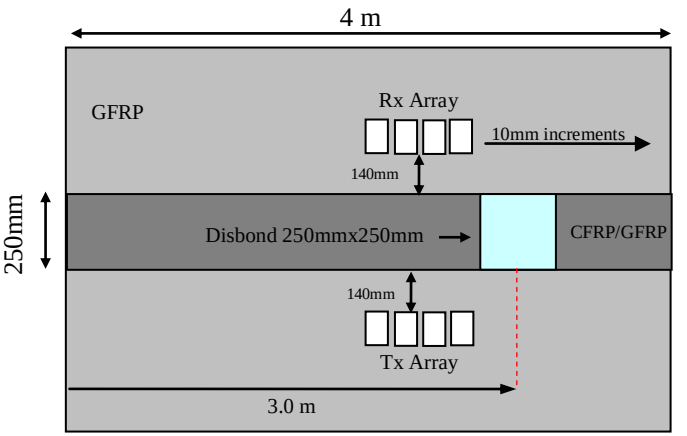

Figure 10: Disbond in spar-cap of blade sample

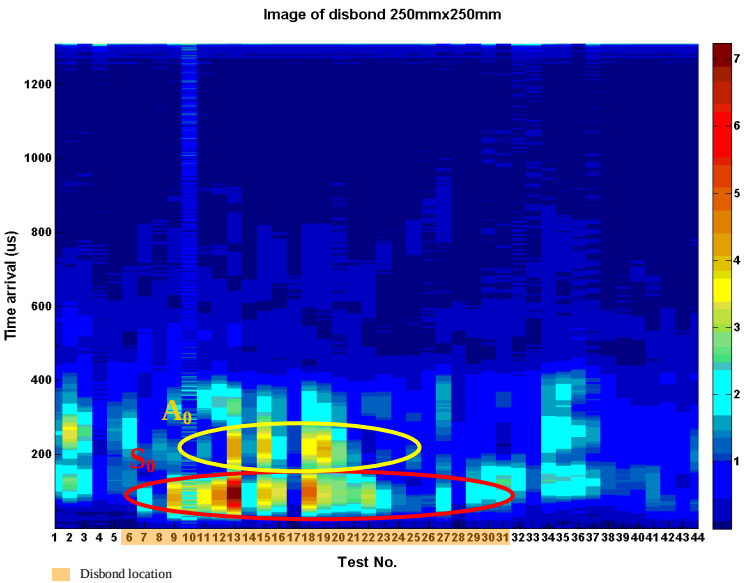

Figure 11: Image of disbond 250mmx250mm

REFERENCE LIST

[1] Executive Committee for the Implementing Agreement for Co-operation in the Research, Development, and Deployment of Wind Energy Systems of the International Energy Agency, 'IEA Wind Energy Annual Report 2005', IEA, 2006

[2] L.W.M.M. Rademakers et al., 'Assessment and Optimisation of Operation and Maintenance of Offshore Wind Turbines', ECN Wind Energy, http://www.ecn.nl/docs/dowec/2003-EWEC-O_M.pdf

[3] Purslow, D., 'Characterization, Analysis and Significance of Defects in Composite Materials', AGARD Conference Proceedings No. 355, 1983.

[4] Cerbe, B., "Damages to rotor blades and their causes", Wind Turbine Blade Manufacture 2010.

[5] Pereira. M., Mudge, P.J., Brown, C.W., Freire, I.J., 'Field Experience of Long Range Ultrasonic Testing', 6th Conferencia sobre Tecnologia de Equipamentos (COTEQ), Salvador BA, Brazil, August 19-21, 2002

[6] Burnham, K., Pierce, S.G., "Acoustic Techniques fro Wind Turbine Blade Monitoring", DAMAS 2007

[7] Viktorov, I.A., 'Rayleigh and Lamb Waves – Physical Theory and Applications', Plenum Press, 1967.

[8] Brigham, E.O., 'The Fast Fourier Transform And Its Applications', Prentice Hall Signal Processing Series, 1988, Chapter 2, pp233

[9] Rhee S., Lee, J.K., Lee, J.J., 'The group velocity variation of Lamb wave in fibre reinforced composite plate', Ultrasonics 47, August 2007, pp.55-63.